13th ewtec 2019 Proceedings of the 13th European Wave and Tidal Energy Conference 1-6 Sept 2019, Naples, Italy

Design and testing of a full-scale 2 MW tidal turbine blade

Edward M. Fagan, Finlay Wallace, Yadong Jiang, Afrooz Kazemi and Jamie Goggins

Abstract—**The Large Structures Research Group of MaREI, Orbital Marine Power Ltd and ÉireComposites Teo. have designed a full-scale blade for a next-generation 2 MW tidal turbine as part of the H2020 FloTEC project. The 8.5 m long blade will be tested under static load conditions through the H2020 MaRINET2 transnational access programme and fatigue conditions through the OCEAN ERA-NET SEABLADE project. This paper provides an overview of the initial design study which analysed the impact of using a single shear web or two shear webs in the design. The result of this design study led to optimisation of the laminates throughout the blade to reduce the cost of manufacture and, hence, the levelized cost of energy of the device. The finite element analyses were performed using the MaREI@NUI Galway composite blade design software BladeComp. From the results of the analyses a single web design was chosen for the blade. The present work also describes the set-up for the structural tests and an overview of the data acquisition and instrumentation requirements for full-scale static and fatigue blade testing.**

Keywords—**Composite blade, structural testing, tidal turbine.**

I. Introduction

DEVELOPMENTS in tidal energy over recent years have seen several companies produce viable utility-scale turbines: the MeyGen project has exported 12 GWh to the grid using 4 1.5 MW Simec Atlantis and Andritz Hydro Hammerfest turbines [1], Minesto have launched a 500 kW tidal kite [2] and Orbital Marine Power have produced 3 GWh in a single year with their twin-rotor 2 MW floating turbine [3]. With production turbines ready for the market, full-scale structural testing of turbine components will be required for several reasons:

1. To validate design processes
2. To inform operation and maintenance procedures
3. To mitigate risk and meet certification standards

Companies will also need to reduce the levelized cost of energy (LCOE) for their production turbines to make tidal energy commercially competitive with onshore wind, offshore wind and solar PV. Structural testing can provide valuable insights into the performance of the blade and blade components, to feed into the iterative design process.

The H2020 FloTEC project is focused on demonstrating an advanced full-scale floating tidal energy system for a low cost of energy [4]. As part of this project, the blades of the new Orbital O2 2 MW rotor will be enlarged, and the device operated at a lower rated speed, to capture 50% more energy than the previous design. The project will also focus on reducing the capital and operational costs of the turbine at the design stage.

As a member of the MaREI Centre, the Large Structures Research Group (LSRG) has developed advanced computational design methodologies for tidal current turbine blades [5], [6], performed design and optimisation studies on wind turbine blade structures of several scales [7]-[9], and conducted structural testing of components for a 3/8th scale blade and rotor subsection for a prototype OpenHydro tidal turbine [10]. The methodologies developed and the research findings on blade structural design and optimisation have been incorporated into an in-house blade design software package called BladeComp. BladeComp was one of the primary tools used in the structural design studies for the new blade for the FloTEC project. Additionally, structural testing for static loading (through the MaRINET2 transnational access programme) and for fatigue loading (through the Ocean Energy ERA-NET Cofund) will be conducted at the Large Structures Testing Laboratory in the Alice Perry Engineering Building at NUI Galway.

This paper presents the results of an initial design study, analysing the optimum structural layout for blade shear webs. The results of this study are discussed and the

Paper ID: 1692, track: TDD

This work was supported in part by the SFI MaREI Centre under grant 12/RC/2302.

E. M. Fagan is with the Department of Civil Engineering, National University of Ireland Galway, University Road, Galway, Ireland, H91 TK33 (e-mail: edward.fagan@nuigalway.ie).

F. Wallace is with Orbital Marine Power Ltd, Innovation Centre – Orkney, Hatston Pier Road, Kirkwall, Orkney, Scotland, KW15 1ZL (e-mail: f.wallace@orbitalmarine.com).

Y. Jiang is with the Department of Civil Engineering, National University of Ireland Galway, University Road, Galway, Ireland, H91 TK33 (e-mail: yadong.jiang@nuigalway.ie).

A. Kazemi is with the Department of Civil Engineering, National University of Ireland Galway, University Road, Galway, Ireland, H91 TK33 (e-mail: a.kazemi@nuigalway.ie).

J. Goggins is with the Department of Civil Engineering, National University of Ireland Galway, University Road, Galway, Ireland, H91 TK33 (e-mail: jamie.goggins@nuigalway.ie).

details of the upcoming testing programme for the full-scale blade is described. The FE analyses and the detailed test setup description presented in this paper are revised and edited from two reports created by NUI Galway for the FloTEC and SEABLADE projects [11], [12].

II. Blade and FE Model Definition

The blade geometry is defined by the chord, twist and airfoil distributions along its length. Fig. 1 displays the chord length and hydrodynamic twist angle for the tidal turbine blade assessed in this study. The material used to construct the blade is a glass-fibre epoxy combination known as "powder epoxy" designed by the manufacturing partners, ÉireComposites Teo. The powder epoxy technology has been experimentally investigated for tidal turbine applications [13] and used to manufacture wind turbine blades [14]. One of the primary advantages of powder epoxy is its manufacturability. Each section of the blade structure (the upper and lower halves and the shear web) can be partially cured, assembled and then fully cured as a single piece without the need for bond lines, typical of other blade manufacturing procedures. Further details of the manufacturing processes for powder epoxy can be found in Flanagan et al [14]. The material properties of unidirectional and biaxial laminates are provided in Table 1. These properties, along with the geometric properties, are used as inputs to BladeComp for generating the blade finite element (FE) models.

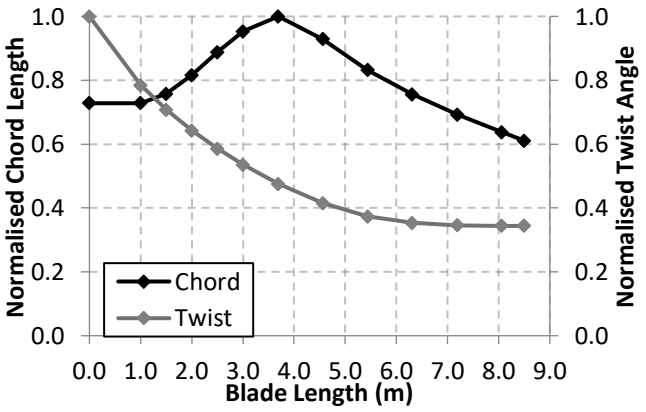

Fig. 1. Chord length and hydrodynamic twist angle distributions along the length of the blade, normalised by the maximum value of each variable.

For the initial analysis of the effect of alternative shear web combinations on the design, a simplified layup for the blade was assumed. The spar and root regions of the blade consisted of layers of biaxial material on the inner and outer surfaces and a solid section of unidirectional laminate in between. The hydrodynamic shells consisted of just biaxial laminates oriented at ±45° to the pitch axis of the blade. Similarly, the webs consisted of just biaxial laminates. Table 2 outlines the distribution of laminate thicknesses along the length of the blade for these three key regions.

Five load cases were considered for the blade, relating to: the maximum flatwise bending moment ($M_{y,max}$), the maximum flatwise shear loading ($F_{y,min,}$), the maximum pitching moment ($M_{z,max}$), the minimum pitching moment ($M_{z,min}$) and a damage equivalent load case (DEL). The load distribution for each case consists of an edgewise and flatwise distribution oriented parallel and perpendicular to the rotor plane, respectively. Fig. 2 shows the distributions of the two components along the blade for the five load cases. The loads are applied in the FE models as multi-point constraints. The nodes in each blade section are coupled to a reference node for that section. The loads from Fig. 2 are applied as point loads to these reference nodes.

TABLE 1
YOUNG'S MODULI, POISSON'S RATIO AND DENSITY USED IN THE FEA

Laminate	E_{11} (MPa)	E_{22} (MPa)	ν_{12}	G_{12} (MPa)	ρ (kg/m³)
UD	38,805	12,785	0.26	3,670	1950
BIAX	25,944	25,944	0.13	3,670	1950

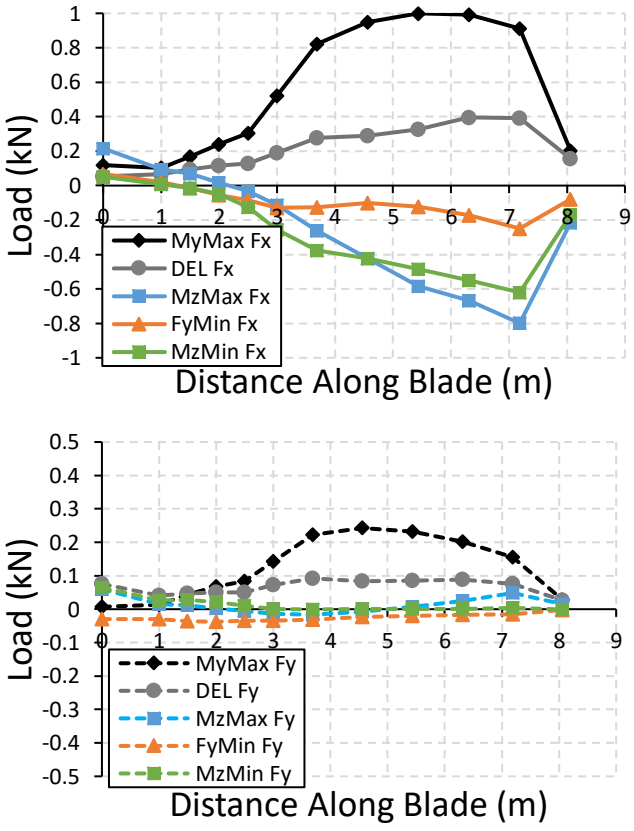

Fig. 2. The flapwise (Fx) and edgewise (Fy) loading distributions for the five load cases, normalised by the maximum static flapwise load.

Static FE analyses were conducted with a total mesh size of approximately 17,000 nodes. This resulted in a typical element length of approximately 50 mm. Reduced integration S4R elements were applied to the model, after a comparison of preliminary results with higher order S8 elements indicated sufficient mesh density for the analyses.

TABLE 2
LAYUPS APPLIED IN EACH SECTION OF THE BLADE MODEL FOR SPAR CAP, OUTER HYDRODYNAMIC SHELL AND SHEAR WEB REGIONS ALONG THE BLADE

Location	**0**	**1**	**2**	**3**	**4**	**5**	**6**	**7**	**8**	**9**	**10**	**11**	**12**
Spars													
BIAX	9	9	9	9	9	9	9	9	9	9	9	9	9
UD	104	84	64	50	50	50	50	45	40	40	35	30	25
BIAX	9	9	9	9	9	9	9	9	9	9	9	9	9
Shells													
BIAX	9	9	9	18	18	18	18	18	18	18	18	18	18
UD	104	60	20										
BIAX	9	9	9										
Web(s)													
BIAX	20	20	20	20	20	20	20	20	20	20	20	20	20

III. SHEAR WEB STUDY

A. Study overview

The primary variable under consideration in the present study was the number of shear webs used in the blade. With a single shear web the main structural member of the blade is formed by an I-beam, while with the double web configuration the spar is formed from a box-beam.

The two structures were modelled and analysed for their deflection, rotation and strains throughout the blade. The strains in biaxial and unidirectional materials were inspected for regions including: the spar cap on the lower (pressure) side of the blade, the spar cap on the upper (suction) side of the blade, the leading edge on the upper and lower sides of the blade, the trailing edge on the upper and lower sides of the blade and the shear web(s) (see Fig. 3). BladeComp allows outputs of strain/stress for each of these locations along the blade, processing all the elements in the region to return the maximum/minimum stresses in each. The results of the strain for the three in-plane components were analysed throughout the blade. Additionally, the results of the five load cases were combined to form maximum and minimum strain envelopes for each location in the blade.

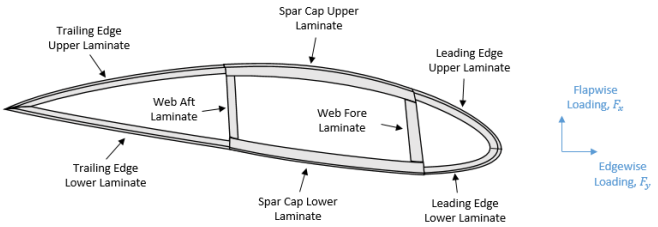

Fig. 3. Naming convention for each region in the blade cross-section.

B. Study results

The results of the longitudinal strain in several regions of the lower spar cap is shown in Fig. 4. Fig. 4 (a) shows the distribution of strain in the innermost biaxial layer for both the Single and Double Web designs, Fig. 4 (b) shows the distribution of strain in the outermost (highest stressed) UD layer for both designs and Fig. 4 (c) shows the distribution of strain in the biaxial layer on the blade surface for both designs.

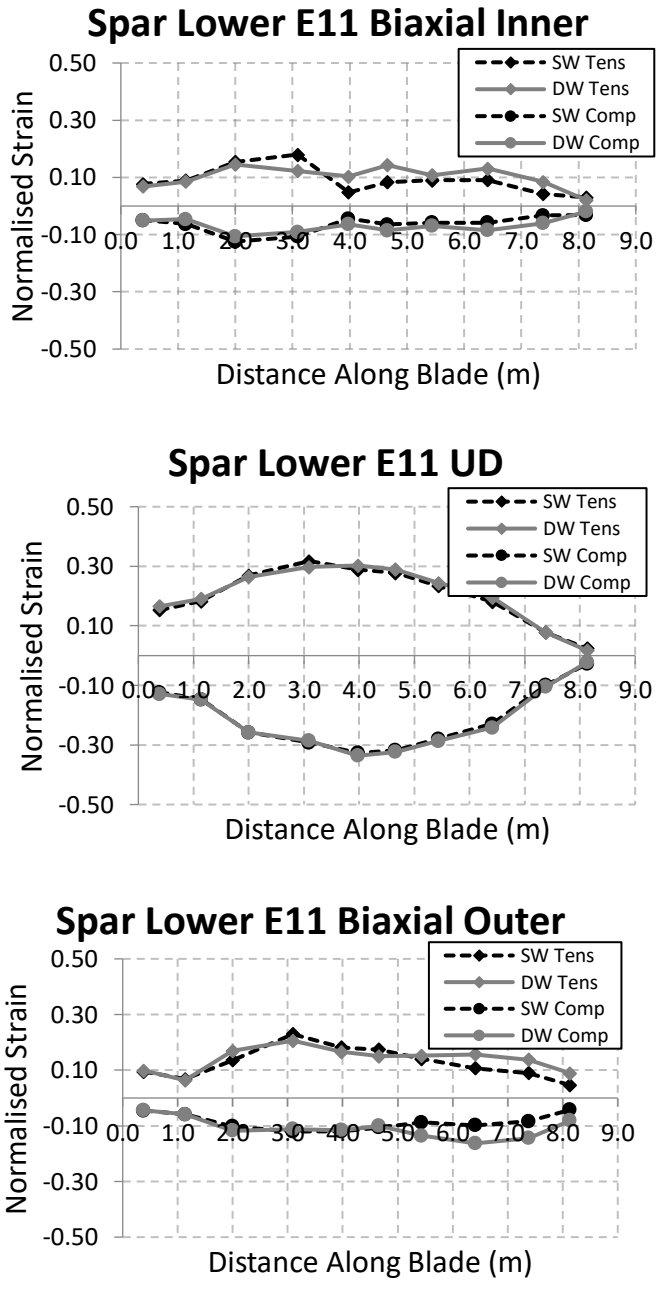

Fig. 4. The maximum longitudinal normalised strain along the blade for (a) the innermost biaxial layer on the pressure side spar cap, (b) the outermost unidirectional layer on the pressure side spar cap, (c) the outermost biaxial layer on the pressure side spar cap.

Fig. 5 compares the maximum strain distributions in the shear web(s) for both blade designs. The results of all 5 load cases were combined to find the maximum strain envelopes for the blade for both Fig. 4 and Fig. 5. The strains reported are normalised by the allowable strains for tension and compression for both UD and biaxial materials. Fig. 6 shows the resultant deflection of both designs at several points along their lengths.

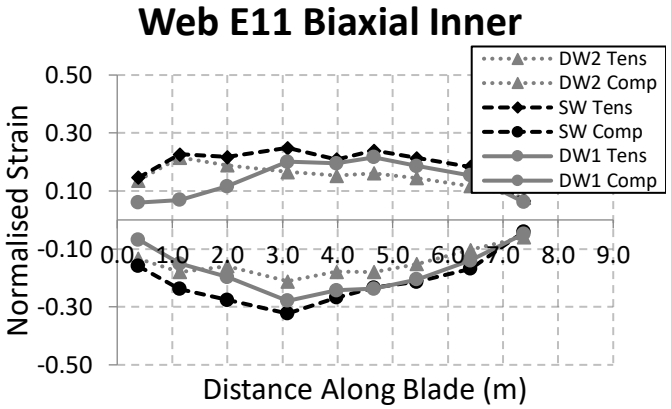

Fig. 5. The longitudinal strain along the blade in the highest loaded biaxial layer in the shear web(s) for both the Single and Double Web designs.

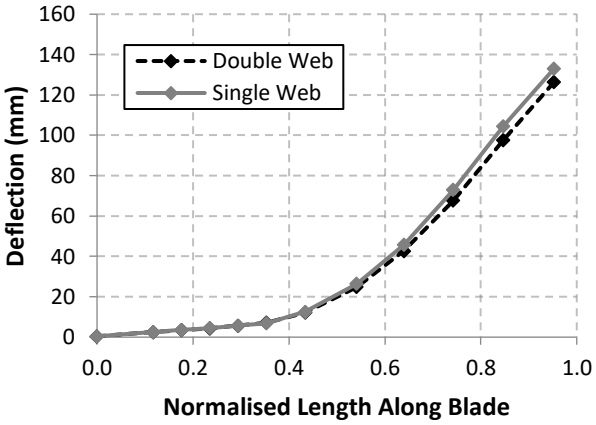

Fig. 6. The resultant deflection of both blade designs.

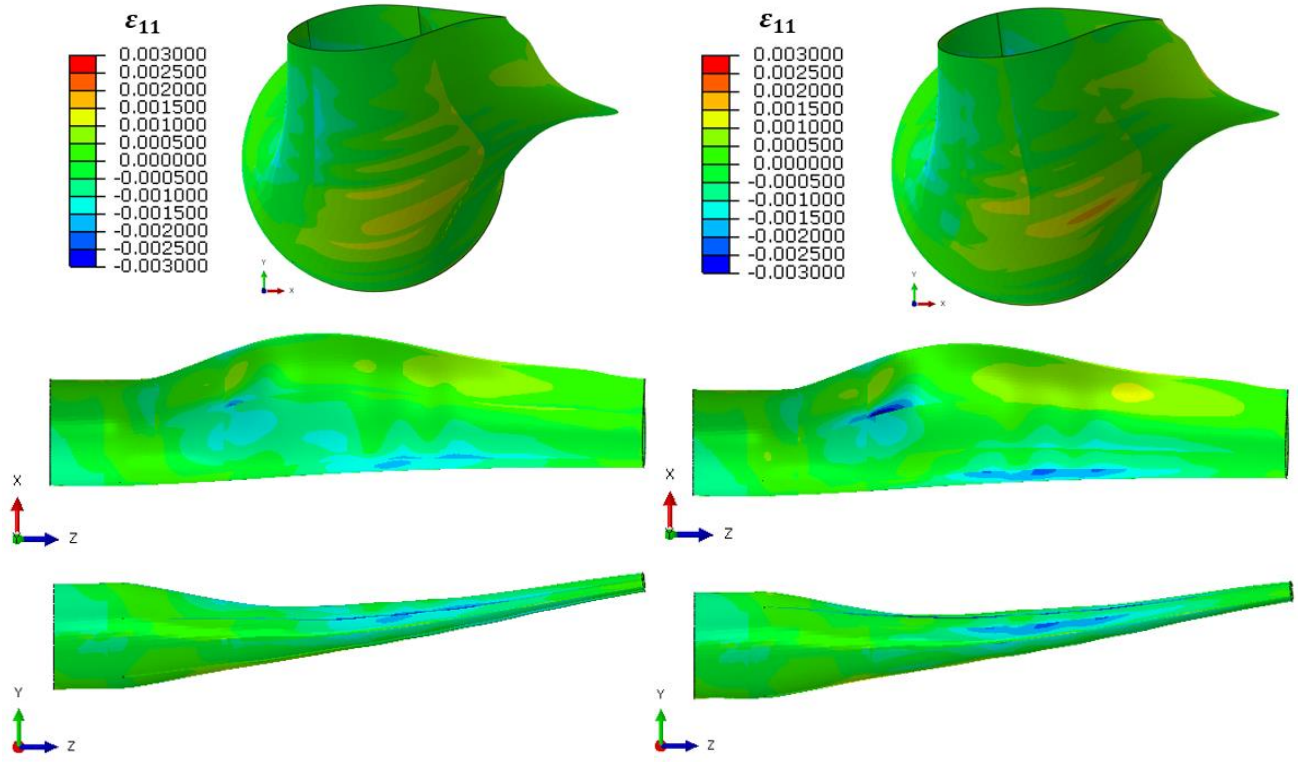

Fig. 7. The Double Web (DW) model longitudinal strain results for the outermost biaxial plies [left] and the Single Web (SW) model longitudinal strain results for the outermost biaxial plies [right].

TABLE 3
SUMMARY OF FINDINGS COMPARING THE SINGLE WEB (SW) AND DOUBLE WEB (DW) BLADE DESIGNS FOR ALL FIVE LOAD CASES COMBINED.

Region	ε_{11}	ε_{22}	ε_{12}
Leading Edge Lower	Minimal difference	Slight increase for SW	Increase for SW
Leading Edge Upper	Slight increase for SW	Slight increase for SW	Increase for SW
Trailing Edge Lower	Slight increase for SW	Slight increase for SW	Slight increase for SW
Trailing Edge Upper	Slight increase for SW	Slight increase for SW	Slight increase for SW
Spar Caps Lower Biaxial	Slight increase for DW	Increase for DW	Slight increase for SW
Spar Caps Upper Biaxial	Slight increase for DW	Increase for DW	Slight increase for SW
Spar Caps Lower UD	Minimal difference	Minimal difference	Increase for DW
Spar Caps Upper UD	Minimal difference	Redistribution	Increase for DW
Shear Webs	Slight increase for SW	Increase for SW	Redistribution

C. Discussion

The figures in the previous subsection demonstrate the effect of using a Single Web (SW) or Double Web (DW) design for the blade. Fig. 4 shows the distribution of the fibre-direction strain along the length of the blade spar caps, comparing the two blade designs. Fig. 4 (b) indicates that the choice of one or two webs has minimal effect on the longitudinal strain in the spar caps of the blade for the UD layers. For the biaxial layers on the inner and outer surface of the blade (Fig. 4 (a) and (c) respectively) the Double Web design shows a slight increase in the tensile and compressive strains from approximately 4 m along the blade to the tip. The strain values in the figures are normalised by the allowable strains for tension and compression for the UD and biaxial materials. The figures indicate the strains are well within margins of safety for both materials. The driving load case for the analyses was the fatigue damage equivalent load (DEL).

Fig. 5 shows the strain distributions in the shear webs of both designs. The web towards the leading edge of the blade is designated DW1 and the trailing edge web DW2, in the figure. The Single Web model demonstrates slightly higher strains than the Double Web model along the blade, peaking at the 3 m location. The strain in the DW1 web is nearly equal to the Single Web model from approximately 3 m to the tip. The peak value of strain occurs at approximately the same location as the Double Web model. The DW2 web shows higher strains than the DW1 web up to the 2 m location, after which the strains decrease along the blade length. The values of the longitudinal strains remain significantly lower than the allowable strains.

Only the longitudinal strains are reported in this paper. However, the results of the transverse and shear strain distributions were also analysed and presented as supplementary material to the original report [11]. The results of the analyses for the seven regions of the blade (Leading Edge Upper and Lower, Trailing Edge Upper and Lower, Spar Caps Upper and Lower and the Shear Webs) and for all three strain components are summarised in Table 3. The results in the table indicate that the most significant differences between the strains in the two blade designs occur for the shear strains, most notably in the leading edge and spar cap laminates. The summary indicates that the shear strains are distributed differently in the blade between the two designs, indicating increases in the spar cap shear strains in the Double Web design, but increases in the trailing edge shear strains in the Single Web design. The values of the shear strains are below the allowable limits for UD and biaxial materials, respectively, for all of the laminates except the leading edge laminates in the Single Web model. This location will be a focus for further analysis in the next stage of the blade design process. For the Single Web model the shear strain in the webs exceeds the allowable strain from approximately 4 m to 7 m along the blade. The thicknesses of the webs, however, is quite low at 20 mm for the Single Web blade in this study.

Fig. 6 shows the difference in the deflection of the two blade designs. The overall tip deflection is within approximately 5% for the two designs. The rotation of the tip of both blade designs was less than approximately 1°.

Fig. 7 shows contour plots of the longitudinal strain component for both blade designs. The strain in the outermost biaxial plies in the blade is shown. The large deformation scale factor highlights the rotation and deflection of the blade along its length for the two designs. The top view in Fig. 7 shows how the Single Web design has resulted in the concentration of the tensile strain in the spar cap towards the trailing edge of the blade, whereas the strain is more evenly distributed across the width of the spar cap in the Double Web model. The middle and bottom views also highlight the increase in strain in the leading and trailing edge laminates with a Single Web design. The results of this preliminary design study indicated the regions of risk and uncertainty in the design that were addressed in the subsequent blade laminate optimisation task of the FloTEC project.

In this optimisation task, the regions of the blade with high strains (noted in the SW plotlines in Fig. 4 and Fig. 5) were addressed in particular to ensure an even strain distribution across the blade within safety margins. This resulted primarily in increased laminate thicknesses and optimised layup drop rates along the blade.

D. Summary

While the strains in various regions of the blade were redistributed due to the overall change in stiffness of the load-carrying blade spar, the resultant strains were well below the failure strains for the material in all regions except the leading edge laminates in the single web model, which requires further study. The strains retained a factor of safety of 2 for the UD spar cap material at a minimum for both designs. The single web design was, therefore, chosen for further analysis, due to its reduced complexity for manufacturing.

IV. Full-scale blade testing

E. Test facility

The facility at NUI Galway for full-scale testing consists of a 375 m² high-bay Large Structures Testing Laboratory. The components of the laboratory relevant to the current testing requirements include:

- Flexible testing spaces that allow for testing small to large structural and mechanical elements and materials.
- 10 m x 6 m strong floor with anchor points at 750 mm to 1000 mm centres each having a capacity of 500 kN.
- Servo-hydraulic testing machines with capacities ranging from 10 kN to 750 kN.

- Hydraulic ring main that allows convenient, efficient test setup, operation, and maintenance of individual test systems without disturbing other systems (working pressure of hydraulic ring main is max 210 bar and with a flow capacity of 300 l/min).

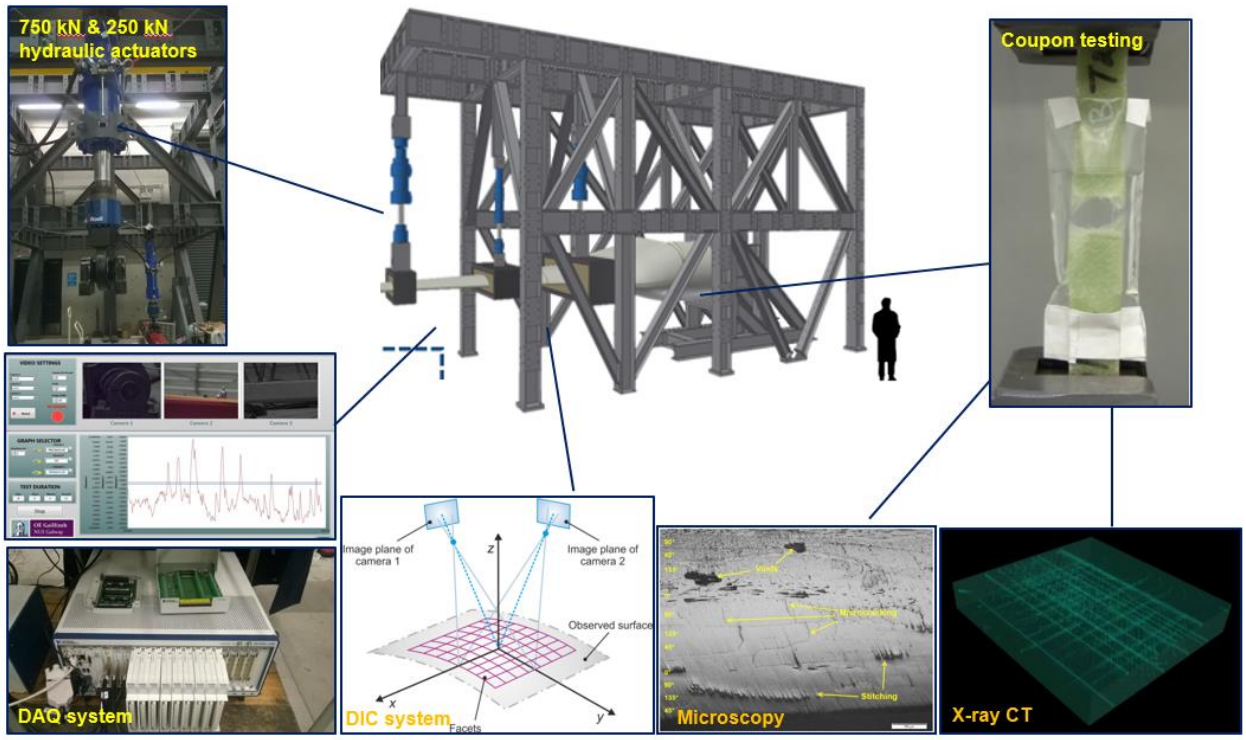

Fig. 8. Testing capabilities of the MaREI Centre's Large Structures Testing Laboratory at the National University of Ireland Galway.

- Data acquisition systems and sensors for measurement of load, deformation, strain and acceleration (covered in detail in Section F).

Fig. 8 shows a computer-generated image of the test setup identifying the major components and capabilities of the laboratory.

F. Test setup

An overview of the test setup is shown in Fig. 9. The blade is supported at its root on a support frame. The support frame is constructed from a steel cylinder providing adequate stiffness and load transferral to 9 bolts on the strong floor.

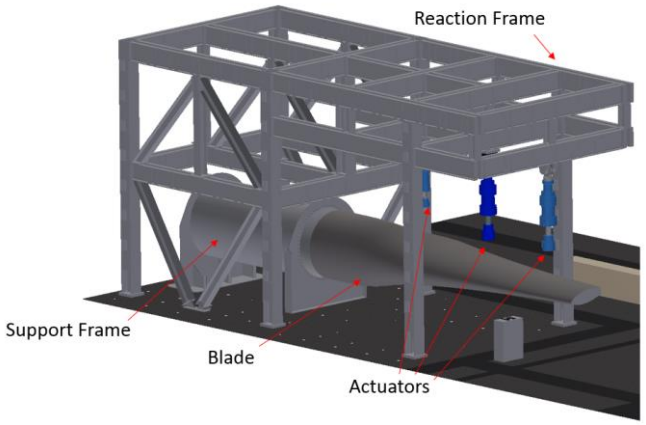

Fig. 9. 3D rendering of the test setup with the main components highlighted.

The blade is loaded via three hydraulic actuators ranging in capacity from 250 kN to 750 kN. In the current setup, the actuators hang from the modular steel frame and apply loads vertically. The three actuators can be controlled separately and in unison for application of complex loading patterns for static and fatigue testing. The load is applied to the surface of the blade through six contact pads and three load introduction mechanisms. The mechanisms split the load from each actuator to two contact pads, thereby doubling the number of loading points and increasing the accuracy of the applied bending moment and shear force profiles along the blade.

G. Instrumentation

This section provides details of the instrumentation available for testing, guidelines on the locations for installing the instrumentation, guidelines on the installation procedure, the technical requirements for testing and details of the acquisition requirements of each type of sensor. The instrumentation includes:

- Electrical resistance strain gauges applied to the surface of the blade.
- Small displacement (LVDTs) and large displacement (draw wire potentiometer) transducers.
- Videometric measurements using Digital Image Correlation (DIC), a 3D laser scanner and a laser scanning vibrometer.

- Load cells at the locations of load application to the blade.
- Accelerometers for natural frequency testing.

Blade deflections of interest include: tip deflection measured in three directions and vertical deflections at up to five other positions along the length of the blade. Measuring the deflections in x- and y-directions at the leading and trailing edges of the blade can also capture the rotational response of the structure. Any deflection of the root support frame or adaptor plate will result in significant parasitic deflections at the blade tip. Hence, it is recommended that the front face of the root attachment fixture is also instrumented. Similarly, the central beam of the reaction frame (upon which the actuators are mounted) should be monitored for vertical deflections.

The non-contact DIC measurement system can provide accurate 3D coordinates, displacements and surface strains. The system consists of two HD stereo cameras. DIC requires a stochastic high contrast pattern to be painted onto the surface of the blade to capture the deformations and strain. Accurate measurements may also require additional lighting within the measurement area. For fatigue testing, the system can be triggered to capture a sequence of images at regular intervals within the testing period.

A Leica ScanStation C10 3D laser scanner is available for measuring the surface geometry of the blade and capturing the entire test setup. The accuracy for a single measurement is 6 mm for position and 4 mm for distance and for a range of 1 m to 50 m a performance of one sigma. The scan rate is up to 50,000 points/sec. The instrument has 80 GB onboard storage. The scanner allows a full 3D point cloud of the test setup to be captured prior to testing. Additionally, at certain points during the test protocol the scanner is employed in a lower resolution mode. For example, when the blade is at full static load, a quick low-resolution scan is performed. Processing the results provides an overlay of undeformed and deformed blade shapes. This methodology can also be used to check the loading direction of the actuators, for high-deflection tests.

A scanning laser vibrometer is also used for testing dynamic phenomena such as vibration levels, mode shape characterisation and obtaining natural frequencies. The system is a PSV-500-B scanning laser Doppler vibrometer (LDV) with associated Polytec PSV software. No surface preparation is required for this device. The device can measure velocity from 0.005 microns/s to 12 m/s across 14 ranges. The device operates within the frequency range of 0 Hz to 100 kHz with a minimum velocity resolution of 0.005 (microns/s)/√Hz and approximately 20 picometre displacement resolution for detecting material damage. Mode shapes in the blade structure can be excited using a speaker setup and multiple scans of the blade can be stitched together to generate a simulation of the mode shapes for the full structure.

The LSRG has a NI PXI-1085 Data Acquisition System with capacity for up to:

- 104 channels to read strain gauges (or strain gauge-based sensors, e.g. load cells, displacement sensors, etc.).
- 16 channels for Linear Variable Displacement Transducers (displacement).
- 8/16 differential/single ended raw Voltage based sensors
- 8 accelerometers.
- Three high definition (HD) cameras.

The system can capture data at up to 20 samples per second, with all data stored locally and backed up to an external hard drive at regular intervals during testing. A comprehensive LabView program for synchronously controlling the experiment and capturing the instrumentation data is also provided by the Large Structures Research Group.

V. Conclusion

This paper describes a design study for a full-scale tidal turbine blade for an Orbital Marine Power 2 MW tidal turbine. The study investigated the impact on the blade structural performance of using one or two shear webs in the design. The designs were assessed by investigating the changes in the distributions of strain and the deflections along the blades. It was found that the impact on blade deflection was minimal when using a single shear web. This preliminary design study acted as the first step towards defining the laminates for the blade. The subsequent optimisation of the blade used the finite element models from this study and the genetic algorithm-based design optimisation functions within BladeComp to optimise the thickness of the composite laminates.

The setup of a full-scale blade test and instrumentation is also described in detail in this paper. Testing of this kind is an important part of the turbine manufacturing process, validating design and modelling work and providing insights into the performance and damage accumulation of the structure under long-term fatigue loading. With many tidal turbine manufacturers having proved the concept for their devices, long-term blade testing will be needed to mitigate risks for their production blades.

Acknowledgement

This material is in part based upon works supported by the Science Foundation Ireland Marine and Renewable Energy Ireland (MaREI) research centre under Grant No. 12/RC/2302. It was also funded by the H2020 FloTEC project and by the Ocean Energy ERA-NET Cofund grant no. 731200. The last author would like to acknowledge the support of Science Foundation Ireland through the Career Development Award programme (Grant No. 13/CDA/2200). Additional thanks are given to the technical staff at NUI Galway and engineering staff at Orbital Marine Power Ltd and ÉireComposites Teo.

REFERENCES

[1] Marine Energy, "Atlantis: MeyGen Reaches 12 GWh Milestone", 20/02/2019 [online]. Available: https://marineenergy.biz/2019/02/20/atlantis-meygen-reaches-12-gwh-milestone/ [accessed on: 27/02/2019].

[2] Marine Energy, "The launch of the world's first subsea tidal kite (Video)" 27/12/2018 [online]. Available: https://marineenergy.biz/2018/12/27/the-launch-of-the-worlds-first-subsea-tidal-kite-video/ [access on: 28/02/2019].

[3] Marine Energy, "Floating tidal turbine clocks record 3 GWh in a single year" 21/08/2018 [online]. Available: https://marineenergy.biz/2018/08/21/floating-tidal-turbine-clocks-record-3gwh-in-a-single-year/ [accessed on: 28/02/2019].

[4] Orbital Marine Power, "FloTEC", Available: https://orbitalmarine.com/flotec/flotec-project/ [accessed on: 28/02/2019].

[5] C. R. Kennedy, S. B. Leen and C. M. Ó Brádaigh, "A Preliminary Design Methodology for Fatigue Life Prediction of Polymer Composites for Tidal Turbine Blades", *Proceedings of the Institution of Mechanical Engineers, Part L, Journal of Materials: Design and Applications*, vol. 226(3), pp. 203-218, 2012.

[6] E. M. Fagan, S. B. Leen, C. R. Kennedy and J. Goggins, "Damage mechanics based design methodology for tidal current turbine composite blades", *Renewable Energy*, vol. 97, pp. 358-72, 2016.

[7] E. M. Fagan, M. Flanagan, S. B. Leen, T. Flanagan, A. Doyle and J. Goggins, "Physical experimental static testing and structural design optimisation for a composite wind turbine blade", *Composite Structures*, vol. 164, pp. 90-103, 2016.

[8] E. M. Fagan, S. B. Leen, O. De La Torre and J. Goggins, "Experimental investigation, numerical modelling and multi-objective optimisation of composite wind turbine blades", *Journal of Structural Integrity and Maintenance*, vol. 2(2), pp. 109–119, 2017.

[9] E. M. Fagan, O. De La Torre, S. B. Leen and J. Goggins, "Validation of the multi-objective structural optimisation of a composite wind turbine blade", *Composite Structures*, vol. 204, pp. 567–577, 2018.

[10] O. De La Torre, D. Moore, D. Gavigan and J. Goggins, "Accelerated life testing study of a novel tidal turbine blade attachment," *International Journal of Fatigue*, vol. 114, pp. 226-237, 2018.

[11] Fagan E. M. and Goggins J., "Single and double web blade modelling", *Research Report No. M.H2020-NUIG-R-001.01*, National University of Ireland, Galway, Ireland, 2018.

[12] E. M. Fagan and J. Goggins, "SR2-2000 Blade Test Procedure", *Research Report No. M.H2020-NUIG-R-005.00*, National University of Ireland, Galway, Ireland, 2018.

[13] P. Alam, D. Mamalis, C. Robert, A. Lafferty and C. O'Brádaigh, "Mechanical properties and damage analyses of fatigue loaded CFRP for tidal turbine applications," Proceedings of the European Wave and Tidal Energy Conference (EWTEC), Cork, Ireland, 2017.

[14] M. H. Flanagan, F. Doyle, E. Fagan, J. Goggins, S. B. Leen, A. Doyle, T. Flanagan and P. J. Feerick, "Large Scale Structural Testing of Wind Turbine Blades Manufactured Using a One-Shot Out-Of-Autoclave Process," Proceedings of the Civil Engineering Research Ireland Conference, Galway, Ireland, 2016.